

Investigation of natural solution effect in electrical conductivity of PANI-CeO₂ nanocomposites

Mohammad Reza Mohammad Shafiee, Ahmad Sattari, Mahboubeh Kargar and Majid Ghashang*

Department of Chemistry, Faculty of Sciences, Najafabad Branch, Islamic Azad University, P.O. Box 517, Najafabad, Iran

(Received May 14, 2016, Revised February 04, 2017, Accepted February 26, 2017)

Abstract. A green biosynthesis method is described for the preparation of Polyaniline (PANI)-cerium dioxide (CeO₂) nanocomposites in different media *via* in-situ oxidative polymerization procedure. The effect of various media including use of HCl, Lemon Juice, Beverage, White Vinegar, Verjuice and Apple vinegar extracts on the particles size, morphology as well as the conductivity of PANI-CeO₂ nanocomposites was investigated. The electron-withdrawing feature of CeO₂ increases doping level of PANI and enhances electron delocalization. These cause a significantly blue shift of C = C stretching band of quinoid from 1570 cm⁻¹ to 1585 cm⁻¹. The optical properties of the pure material and polymeric nanocomposites as well as their interfacial interaction in nanocomposite structures analyzed by UV-visible spectroscopy. The DC electrical conductivity (σ) of as-prepared HCl doped PANI and a PANI-CeO₂ nanocomposite measured by a four-probe method at room temperature was studied.

Keywords: natural solution; PANI-CeO₂; nanocomposite; in situ oxidative

1. Introduction

Conducting polymers, metal oxides, and different carbon morphologies are a good candidate for fabrication of supercapacitors, rechargeable batteries, electromagnetic interference shielding, displays, Electrochromic materials, artificial muscles and chemical sensors (Lin *et al.* 2013, Zhou *et al.* 2012. Their long time life, easy mode of performance, fast switching speed, and high storage capacity of this kind of polymers have reached more attention (Pech *et al.* 2010). Among the other conducting polymers polyaniline (PANI) has been extensively studied because of its unique features such as high conductivity, high theoretical capacitance, eco-friendly nature, durability, and easy preparation procedures Kumar and Baek (2014). One of the best ways to take advantage of this polymer's unique property is nanotechnology. The large specific surface areas of polyaniline nanoparticles enhance their response to external stimuli rather than bulk polymer (Weiss *et al.* 2004).

Despite unique features, the poor electrical stability of these polymers towards Electrochromic metal oxides limits their usage in different applications. One of the best ways to solve this problem is the preparation of nanocomposites comprised of conducting polymer matrices and metal-oxides in various morphologies such as nanotubes, nanofibers, and hierarchical structures instead of bulk polymer. Results from more studies and several groups work in this field demonstrated that nanocomposites have better optical properties than bulk metal oxides and better

stability than polymer matrices. Incorporation of electron acceptor metal oxides such as CeO₂ (Ghosh *et al.* 2014a, b, 2015) with polymer matrices and followed by provide electron donor-acceptor pairs improve modification of these materials compositionally and morphologically (Gemeay *et al.* 2005, Du *et al.* 2004, Anothumakkool *et al.* 2013). On the hands, composite materials are of great interest as they are applicable in a broad range of mechanical engineering, catalysis and other industrial applications (Aghaei *et al.* 2015, Afnani and Erkmen 2016).

Various techniques regarding the incorporation of nanoparticles into the polymeric matrices such as PANI have been developed in many investigations. In some of these cases all of the ingredients, mix or blend with each other and produce a polymer in solution or mild form. In some other cases, nanocomposites have been synthesized by electrochemistry or wet chemistry using soft or hard templates (Tsai *et al.* 1997). On the other hand, interfacial polymerization, nanofiber seeding are examples of the template-less nanocomposite preparation techniques. Among these methods, the introduction of inorganic nanoparticles into the polymer matrix by chemical route provides materials with new dimensions of characteristics such as catalytic property, magnetic susceptibility, colloid stability (Zhang *et al.* 2004). In the case of PANI nanocomposites, PANI gain unique tunable conductivity either is protonic acid doping or redox doping, but it can be retained electrically active only in PH below three. Many investigations have been published to modify the decreased applications of this kind of polymer because of this problem. In most of the cases, PANI has been doped based on protonic acid mechanisms in natural and alkaline media to be active electrically. Electroactive PANI also has been synthesized by means of organic and inorganic nano-

*Corresponding author, Ph.D., Professor,
E-mail: ghashangmajid@gmail.com

particles such as gold nanoparticles and carbon nanotubes in natural media.

PANI-CeO₂ nanocomposites have been used extensively as gas sensing materials (Khened *et al.* 2016), a potential inhibitor for mild steel in an acidic environment in industries (Sasikumar *et al.* 2015), and hydrogen peroxide (H₂O₂) sensors (Ansari *et al.* 2009).

In continue of our investigations (Shafiee *et al.* 2013, 2012, Taghrir *et al.* 2016, Ghashang *et al.* 2015, 2014, Ghashang 2012, Dehbashi *et al.* 2013), we report a simple, affordable and an eco-friendly method to synthesize electroactive PANI-CeO₂ nanocomposites in natural solutions. Electroactivity of PANI would be improved by in situ polymerization of water soluble aniline monomer in the presence of CeO₂ nanoparticle that is electro-active because of the fast electron transfer. The effect of different natural solutions in doping level of PANI-CeO₂ nanocomposite followed by its electrical conductivity and ultraviolet absorbance has clarified in more details.

2. Experimental

2.1 Materials

Aniline monomer (99%), Ammonium persulfate, (NH₄)₂S₂O₈ (98%), Cerium (III) nitrate hexahydrate (CeN₃O₉.6H₂O, 99.5%) and Ammonia solution (NH₄OH, 37%) were purchased from Merck. We also used some naturally prepared solvents such as Lemon juice, Beverage, white vinegar, Verjuice (the juice of unripe grapes) and Apple vinegar to make samples. The bitter orange leaf juice was prepared in the laboratory. Hydrochloric acid (37%, Merck), Ethanol (98%) and Distilled water were used as received.

2.2 Preparation of bitter orange leaf

Bitter Orange leaves (200 g) were washed in running tap water, and then mixed with ethanol (200 mL) and distilled water (600 mL) up to 4 h on the magnetic stirrer at 100-120°C. A small amount of the extract (100 mL) was used for the synthesis.

2.3 Green synthesis of CeO₂ nanoparticles

At first, 100 g of Leaves of Bitter Orange Leaf were ground and inserted in a 1000 balloon flask containing 600 mL of deionized water and 200 mL of ethanol and the mixture was refluxed for 4h. Afterward, the extract was filtered to cut off the unrequited bodies. 200 mL of extract was combined with 20 mL of aqueous ammonia (37%).

Next, the prepared solution was pureed dropwise to an aqueous solution of cerium (III) nitrate hexahydrate (prepared by dissolving of CeN₃O₉.6H₂O (25 mmol) in 300 mL of water) under vigorous magnetic stirring. Next, the resulted mixture was aged for 2 h until a precipitate was formed. Finally, the mixture was filtered washed with water for three times, dried and calcinated at 300°C for 2 h in an electric furnace using alumina crucibles and maintained at the stable mentioned temperature for 2 h. After calcination, the obtained yellow products of CeO₂ were stored in air

tight container for further analysis.

2.4 Preparation of PANI- CeO₂ nanocomposites

In situ oxidative polymerization is an efficient method to prepare PANI- CeO₂ nanocomposite in natural solutions. In this way, 816 mg CeO₂ nanoparticle was dispersed in 25 mL Lemon juice in a round bottom flask. Then 1.825 mL aniline monomer was added to above mixture and stirred for 30 minutes to prepare a homogeneous solution. After that ammonium persulfate solution (2.282 g APS in 12.5 mL Lemon juice) was added to the above mixture drop by drop and the polymerization was allowed to proceed for 24 hours at room temperature. The reaction mixture was filtered and washed with the distilled water and ethanol, respectively, until the filtrate would be colorless. Afterward, the product was dried in a vacuum oven at 100°C for 12 hours to give a delicate tint green powder. In other samples, all of the steps were as above, in addition to using some other natural solution such as Apple vinegar, white vinegar, Beverage and Verjuice instead of Lemon juice. When 25 mL 0.8 mol/L HCl aqueous solution was also used to prepare PANI-CeO₂ nanocomposite instead of natural solutions for comparison, the require time for polymerization was 2 hours instead of 24 hours.

3. Characterization

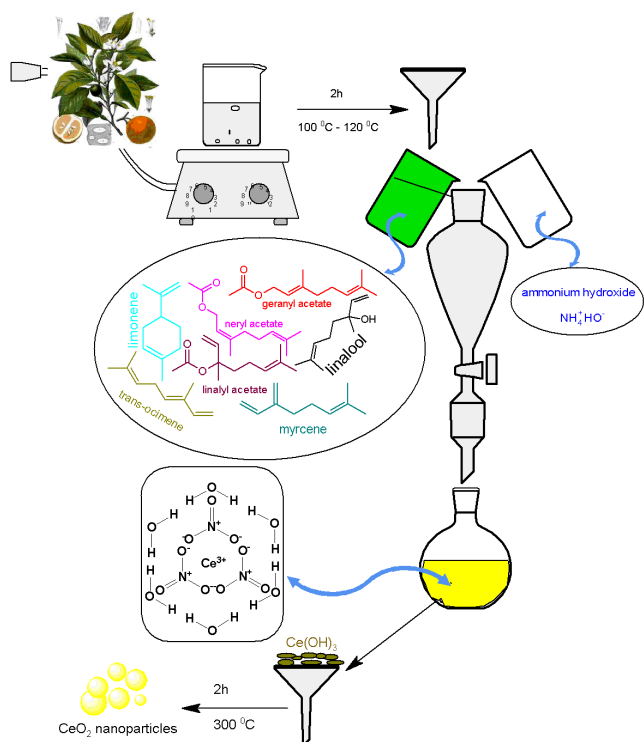
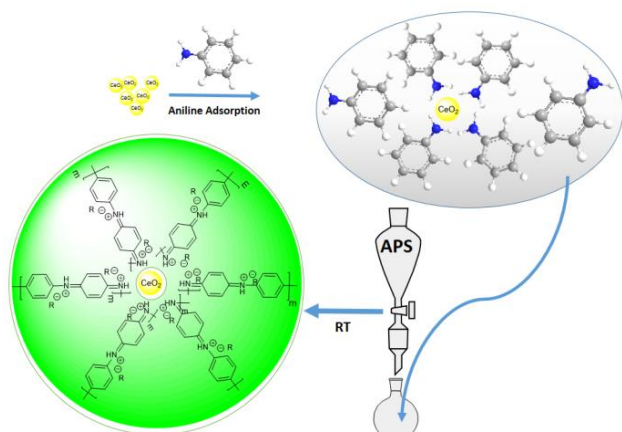
Phase identification was carried out by the as-precipitated and heat treated samples by an X-ray Diffraction (XRD) method with a Rigaku D-max C III, X-ray diffractometer using Ni-filtered Cu K α radiation. Field Emission Scanning Electron Microscope (FE-SEM) images were obtained on HITACHI S-4160. Fourier transform infrared (FT-IR) spectra were recorded on JASCO, 6300 spectrophotometers in solid phase using the KBr pellets technique in the range of 3500-400 cm⁻¹. The UV-visible spectra of the solid materials were obtained with a JASCO V-670 UV-Visible spectrometer. The UV wavelength range was from 900 to 190 nm. The electrical conductivity of the dried composite pellets was measured by a four-point probe method using a Keithley 2001 electrometer.

4. Result and discussion

4.1 CeO₂nanoparticle and CeO₂- PANI nanocomposite preparation

Green synthesis of CeO₂ nanoparticles is illustrated in Fig. 1 (Kargar *et al.* 2015). In this eco-friendly synthesis, the juice of Bitter orange leaf was used. Some of the main components of the juice are illustrated in the Fig. 1. Bitter orange leaf is reached from the essential oils such as oxygenated monoterpene and hydrocarbonated monoterpene. These chemicals can act as a surfactant agent (Azhdarzadeh and Hojjati 2016). The effect of these organic materials in the morphology of as-prepared nanoparticles is apprehensible from FE-SEM in Section 4.4.

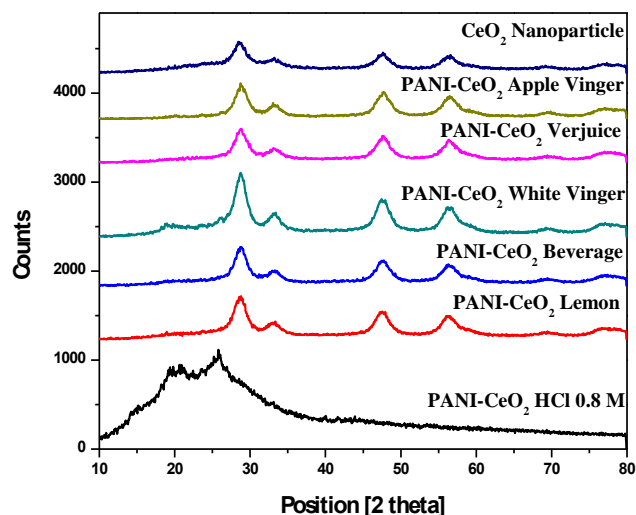
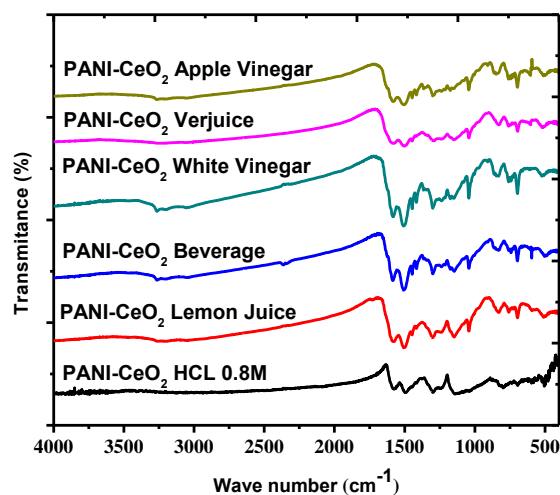
Fig. 2 shows the one-pot synthesis of PANI-CeO₂ nanocomposites. A likely mechanism is in situ polymerization of

Fig. 1 Green synthesis of CeO₂ nanoparticlesFig. 2 CeO₂-PANI nanocomposite synthesis illustration in different mediums. R⁻ shows the type of anion from hydrolysis of various solution acidic components

aniline monomers adsorbed on the surface of CeO₂ nanoparticles. It is worthy of noting that the amount of aniline could adsorb on the surface of CeO₂ nanoparticles as nuclei, different ingredients influence UV-visible absorbance, doping level and crystallinity of PANI chains of as-prepared composites. Most of the active acidic components of these solutions are listed in the appendix. Their coherent effect on the above-mentioned composite properties unrevealed in the result section.

4.2 XRD patterns

The correct crystallinities of CeO₂ nanoparticles and

Fig. 3 XRD spectra of pure CeO₂ nanoparticle and PANI-CeO₂ composites prepared in different mediaFig. 4 FT-IR spectra of PANI-CeO₂ composites in different medium

CeO₂-PANI nanocomposite are shown in Fig. 3. The XRD pattern of the CeO₂ nanoparticle (navy curve) is in good accordance with single phase cubic structure (space group Fm3m), with lattice parameter $a = 5.4110\text{\AA}$ (JCPDS 00-004 0593). In general, diffraction pattern can show a peak broadening owing to the effects of particle size which is around 12 nm according to the Debye-Scherrer formula. It is worthy to note that the diffraction pattern of CeO₂-PANI nanocomposite, indicating that PANI is amorphous in the composite. PANI is adsorbed on the surface of a nano-CeO₂ particle, PANI molecular chain growth is restricted along with decreasing of crystalline and the diffraction peaks gradually disappear (Kowsari and Faraghi 2010).

4.3 FTIR spectroscopy

The chemical structure and functional groups of synthesized materials are unraveled using Fourier transform infrared (FT-IR) spectra analysis. The FT-IR spectra of

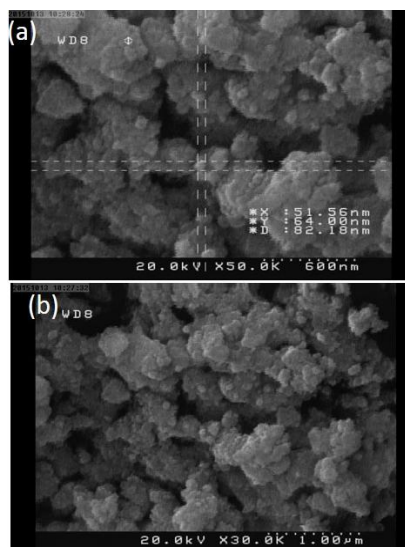


Fig. 5 SEM images of CeO₂ nanoparticles in (a) 50.0K; and (b) 30.0K

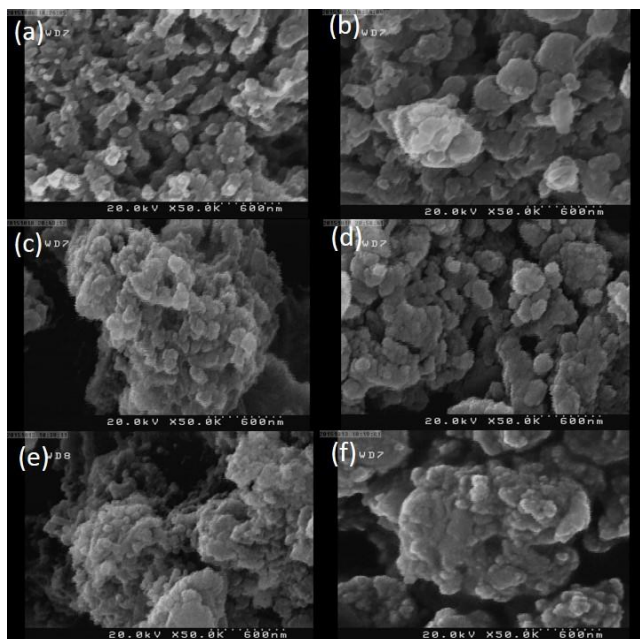


Fig. 6 SEM images of the PANI-CeO₂ nanocomposite in (a) HCl 0.8 M; (b) Lemon Juice; (c) Beverage; (d) White Vinegar; (e) Verjuice; and (f) Apple vinegar

PANI-CeO₂ nanocomposites prepared in different media are shown in Fig. 4. From the spectra, the peaks in the 511 cm⁻¹ and 594 cm⁻¹ are possibly related to (Ce-O) stretching band for CeO₂ materials and metal – oxygen bond is observed at 835 cm⁻¹ (Taguchi *et al.* 2011, Sasikumar *et al.* 2015). The band at around 3265 cm⁻¹ mainly is related to –NH stretching of PANI overlapped by O-H stretching vibration of residual water and hydroxyl groups (Yan *et al.* 2012). The characteristic bands of PANI occur at 1585 cm⁻¹ and 1475 cm⁻¹ (C = C stretching of quinoid and benzenoid), 1508 cm⁻¹ (C = N stretching N = Q = N), 1400 cm⁻¹, 1299 cm⁻¹ and 1245 cm⁻¹ display C-N stretching mode

of benzenoid and quinoid rings. It is noted that electron-withdrawing feature of CeO₂ increases is doping level of PANI and enhances electron delocalization. These causes significantly blue shift of C = C stretching band of quinoid from 1570 cm⁻¹ to 1585 cm⁻¹ (Xiong *et al.* 2010). If CeO₂ bonded covalently to PANI, such strong interactions would occur. The CeO₂ content in synthesized nano-composite affect the FT-IR results.

4.4 SEM Images

SEM images characterized the morphological features of as-prepared PANI-CeO₂ nano-composites. SEM images of green synthesized CeO₂ nano-particles, Figs. 5(a) and (b), demonstrate nearly spherical shaped particles by a large agglomeration and the average size of 25 nm Chuang and Yang (2008). As alkali power of NH₄OH is less than NaOH, the time need for hydrolysis process would be increased, and this not only higher the size of nanoparticles but also enhance their agglomeration rate. It is also confirmed from images that some of the nano-particles are slightly elongated, which is because of the possibility of different atomic density that provides different crystallographic planes. We could also observe nanoparticles agglomeration because of CeO₂ particle tendency to lower the surface energy. Fig. 6 presents SEM images of PANI-CeO₂ nanocomposites prepared in different media. A cage of PANI which surrounds or caps the mono CeO₂ particle could be viewed in images. As CeO₂ nanoparticle has a nucleus effect during the in situ polymerization of aniline monomers, the morphology of nanocomposite would be homogeneous core-shell type in the range of < 40 nm (Kumar *et al.* 2012). It is indicated from Fig. 5(a), the size and homogeneity of nanocomposites prepared in acidic media are less compared to samples developed in other natural solutions. It can be pierced that as the rate of polymerization is very high and some of the polymeric chains arrange not in the form of shell on the CeO₂ particle cores but the form of net with embedded or dispersed CeO₂ nanoparticles (Phang *et al.* 2008, Jing *et al.* 2007, Mo *et al.* 2008, Jiang *et al.* 2009). On the other hand, it is worth noting that the homogeneity and size of nanocomposites in Figs. 6(b)-(f) would be increased and especially in Figs. 6(c)-(f), the tendency to form cluster morphology could be noticed. This is probably because in natural solutions water molecules were absorbed on the surface of CeO₂ nanoparticles and follow that hydrogen bonds selectively form between these molecules and free aniline monomers and anilinium cations. The formations of these bonds cause PANI preferentially grows on the surfaces of CeO₂ nanoparticles and provides core-shell structures (Gai *et al.* 2009).

4.5 Uv-visible analysis

The optical properties of the pure material and polymeric nanocomposites as well as their interfacial interaction in nanocomposite structures analyzed by UV-visible spectroscopy. From the literature (Poyraz *et al.* 2014), the electron transition peaks of pure PANI were observed at 300-350 nm, 450-500 nm and around 800 nm

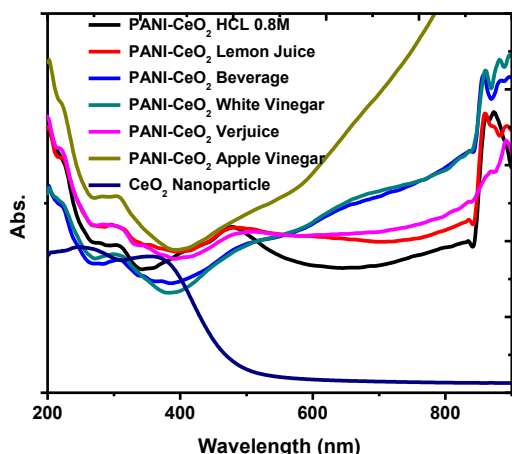


Fig. 7 UV-visible spectra of PANI-CeO₂ nanocomposites and CeO₂ nanoparticles

corresponding to π - π^* , polaron- π^* and π -polaron transitions, respectively. It is noted that π - π^* transition of electrons is related to benzenoid rings in doped PANI (Pillalamarri *et al.* 2005), Boomi and Prabu (2013) and polaron- π^* transition is ascribed to the protonated PANI structure and charge transfer from the benzenoid to the quinoid (Ansari *et al.* 2014), Chiou and Epstein (2005). Later transition, π -polaron transition, is related to the emeraldine base of PANI backbone (Kumar *et al.* 2012, Tamboli *et al.* 2012). Fig. 7 shows the UV-visible spectra of PANI nanocomposite and CeO₂ nanoparticles. Furthermore, as indicated in Figs. 7(a)-(f) most of the as-prepared samples exhibit characteristic absorption peak of PANI which mentioned above. However, the bathochromic shift of PANI-CeO₂ absorption spectra arises from the interaction of CeO₂ nanoparticles with PANI backbone in the form of core-shell structure (Abdullah Dar *et al.* 2012). It is worthy of note that the exciton transition from a localized benzenoid highest occupied molecular orbital (HOMO) to a quinoid lowest unoccupied molecular orbital (LOMO) provide a centered peak at around 650 nm according to Figs. 7(c)-(d) (Gai *et al.* 2009, Stejskal *et al.* 2001). In a comparison of UV-visible spectra of nanocomposites, Figs. 7(a)-(f), with pure CeO₂ nano-particles, Fig. 7(g), two peaks centered at around 220 nm and 290 nm appeared which attributed to the ultraviolet absorption characteristic of CeO₂ nanoparticles. The position and intensities of formed different oxidation state in nanocomposite structure on the CeO₂ nanoparticles are noticeable from different spectra of composites and pure CeO₂ particles. Thus, assigned from optical spectroscopy, the important role of dopant ions size and structure in the formation of insulating and conducting phase in the core-shell structure of prepared nano-composites are inevitable (Kumar *et al.* 2012).

4.6 Conductivity

The DC electrical conductivity (σ) of as-prepared HCl doped PANI and PANI-CeO₂ nanocomposites measured by a four-probe method at room temperature is illustrated in Fig. 8. The overall conductivity of the samples, which

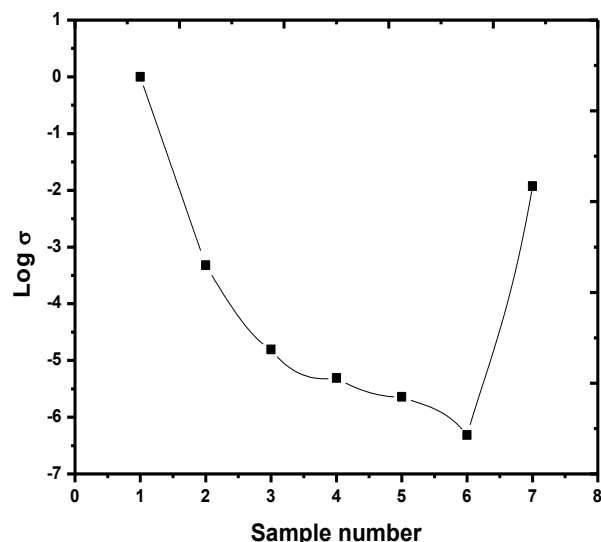


Fig. 7 UV-visible spectra of PANI-CeO₂ nanocomposites and CeO₂ nanoparticles

Table 1 Electrical conductivity (σ) of PANI and PANI-CeO₂ nanocomposites

Number	Sample	Type of solution	Conductivity (S/cm) (error limit $\pm 0.05\%$)	Log σ
1	PANI-CeO ₂	HCl (0.8 M)	1.00E+00	0.00
2	PANI-CeO ₂	Lemon Juice	4.78E-04	-3.32057
3	PANI-CeO ₂	Beverage	1.56E-05	-4.80688
4	PANI-CeO ₂	White Vinegar	4.93E-06	-5.30715
5	PANI-CeO ₂	Grape Verjuice	2.28E-06	-5.64207
6	PANI-CeO ₂	Apple Vinegar	4.85E-07	-6.31426
7	PANI	HCl (0.8 M)	1.18E-02	-1.92812

^a The concentration of aniline monomer, APS as oxidant agent and CeO₂ nanoparticle in parent solutions of all samples were 0.8 M, 0.8 M and 0.16 M respectively. The average of 3 measurements, which were generally within $\pm 10\%$ of each other is conductivity values

changes from conducting materials to insulators was in the range of 1.00 S/cm to 4.85×10^{-7} S/cm in Table 1. The electrical conductivity of HCl doped PANI increased from 0.0118 (S/cm) to 1.00 (S/cm) when aniline monomers polymerized in the presence of CeO₂ nanoparticles as a nucleus. Because the arbitrary molecular chain structures of polymeric materials develop defects like breakings or non-conducting ends, an electron couldn't transmit through chains and conducting process would be inhibited (Sharma *et al.* 2015). In these situations, electron has to find an alternate way to conduct such as hopping, tunneling or passing to a conducting support. In the case of CeO₂ nanoparticles, they couldn't collect electron, but they are believed to act as a more efficient structure for charge transport by hopping or tunneling. In addition, the role of CeO₂ nanoparticles in nanocomposite structure is increasing the compactness of sample, high coupling of grain boundaries. On the other hand, decreasing conjugated length in the PANI chains, which in turn increases the

density and follow that the electrical conductivity of nanocomposite (Ansari *et al.* 2014). There are possibly several reasons why electrical conductivity of as-prepared nanocomposites decreases when the reaction medium changes from acidic to natural solutions:

- (1) The proton doping of PANI shell decreases.
- (2) The hydrolysis of CeO₂ nanoparticle surface increase, so PANI is present as a separate layer and highly aggregated particles are formed (Reddy *et al.* 2008).
- (3) The increased size of the anion in these solutions, as shown in Scheme 2, prevents the adsorption of aniline and anilinium monomers on the surface of CeO₂ nanoparticles on which electrical conductivity depends on.

Besides mentioned reasons, various competing factors such as the plasticizing effect of any traces of washing solvent, the amount of crystalline PANI chains on the shell structures (based on XRD data) and the poor electrical conductivity of CeO₂ nanoparticles influences the electrical conductivity of nanocomposites.

5. Conclusions

In this study, CeO₂ nanoparticles were prepared in a Bitter orange leaf extract and was characterized by XRD and FE-SEM techniques. The XRD pattern of the CeO₂ nanoparticles shows a single-phase cubic structure with a crystal size of 12 nm. The as-prepared CeO₂ nanoparticles were used for the in situ oxidative polymerization synthesis of PANI-CeO₂ nanocomposites, which was characterized, by XRD, FE-SEM, UV-vis and FT-IR techniques. The effect of different media including use of HCl, Lemon Juice, Beverage, White Vinegar, Verjuice and Apple vinegar extracts on the particles size, morphology as well as the conductivity of PANI-CeO₂ nanocomposites was investigated. Polymerization of aniline monomers on the surface of CeO₂ nanoparticles as core provides pseudo-spherical nanocomposites with core-shell morphology. FE-SEM photographs not only reveal the morphology of as-prepared polymeric nanocomposites but also show the size and homogeneity of nanocomposites prepared in acidic media are less compared to samples developed in other natural solutions because of high polymerization rate. The XRD patterns indicate amorphous PANI chains are adsorbed on the surface of nano-CeO₂ particles. The enhanced electron delocalization of PANI is revealed by FT-IR spectroscopy in which electron-withdrawing feature of CeO₂ increases is doping level of PANI. UV-visible spectra have been used to characterize the interfacial interaction between the polyaniline (PANI) chains and CeO₂ nanocrystals. PANI optical properties would be increased by decreasing the highest occupied molecular orbital (HOMO) energy because of electron donor (PANI)-acceptor (CeO₂) interactions. In addition, the DC electrical conductivity of as prepared nanocomposites is explained by a four-probe method. The electrical conductivity of CeO₂ embedded PANI nanocomposites is increased

in comparison to pure PANI because the CeO₂ cores act as a more efficient structure for charge transport by hopping or tunneling instead of electron transmit through PANI chains.

Acknowledgments

We are thankful to the Najafabad Branch, Islamic Azad University research council for partial support of this investigation.

References

- Abdullah Dar, M., Kotnala, R.K., Verma, V., Shah, J., Siddiqui, W.A. and Alam, M. (2012), "High magneto-crystalline anisotropic core-shell structured Mn_{0.5}Zn_{0.5}Fe₂O₄/polyaniline nanocomposites prepared by in situ emulsion polymerization", *J. Phys. Chem. C*, **116**(9), 5277-5287.
- Afnani, A. and Erkmen, R.E. (2016), "Iterative global-local procedure for the analysis of thin-walled composite laminates", *Steel Compos. Struct., Int. J.*, **20**(3), 693-718.
- Aghaei, M., Forouzan, M.R., Nikforouz, M. and Shahabi, E. (2015), "A study on different failure criteria to predict damage in glass/polyester composite beams under low velocity impact", *Steel Compos. Struct., Int. J.*, **18**(5), 1291-1303.
- Anothumakkool, B., Torris, A.T.A., Bhang, S.N., Unni, S.M., Badiger, M.V. and Kurungot, S. (2013), "Design of a high performance thin all-solid-state supercapacitor mimicking the active interface of its liquid-state counterpart", *ACS Appl. Mater. Interfaces*, **5**(24), 13397-13404.
- Ansari, A.A., Sumana, G., Khan, R. and Malhotra, B.D. (2009), "Polyaniline-cerium oxide nanocomposite for hydrogen peroxide sensor", *J. Nanosci. Nanotech.*, **9**(8), 4679-4685.
- Ansari, M.O., Mansoor Khan, M., Ansari, S.A., Raju, K., Lee, J. and Cho, M.H. (2014), "Enhanced thermal stability under DC electrical conductivity retention and visible light activity of Ag/TiO₂@ polyaniline nanocomposite film", *ACS Appl. Mater. Interfaces*, **6**(11), 8124-8133.
- Azhdarzadeh, F. and Hojjati, M. (2016), "Chemical composition and antimicrobial activity of leaf, ripe and unripe peel of bitter orange (*Citrus aurantium*) essential oils", *Nutr. Food Sci. Res.*, **3**(1), 43-50.
- Boomi, P. and Prabu, H.G. (2013), "Synthesis, characterization and antibacterial analysis of polyaniline/Au-Pd nanocomposite", *Colloids Surf. A*, **429**, 51-59.
- Chiou, N.R. and Epstein, A.J. (2005), "Polyaniline nanofibers prepared by dilute polymerization", *Adv. Mater.*, **17**(13), 1679-1683.
- Chuang, F. and Yang, S. (2008), "Cerium dioxide/polyaniline core-shell nanocomposites", *J. Colloid Interface Sci.*, **320**(1), 194-201.
- Dehbashi, M., Aliahmad, M., Mohammad Shafiee, M.R. and Ghashang, M. (2013), "Nickel-doped SnO₂ nanoparticles: Preparation and evaluation of their catalytic activity in the synthesis of 1-amido Alkyl-2-naphthols", *Synth. React. Inorg. Metal-Org. Nano-Metal Chem*, **43**(9), 1301-1306.
- Du, X.S., Xiao, M. and Meng, Y.Z. (2004), "Facile synthesis of highly conductive polyaniline/graphite nanocomposites", *Eur. Polym. J.*, **40**(7), 1489-1493.
- Gai, L., Du, G., Zuo, Z., Wang, Y., Liu, D. and Liu, H. (2009), "Controlled synthesis of hydrogen titanate-polyaniline composite nanowires and their resistance-temperature characteristics", *J. Phys. Chem. C*, **113**(18), 7610-7615.
- Gemeay, A.H., Mansour, I.A., El-sharkawy, R.G. and Zaki, A.B. (2005), "Preparation and characterization of polyaniline/

- manganese dioxide composites via oxidative polymerization: effect of acids”, *Eur. Polym. J.*, **41**(11), 2575-2583.
- Ghashang, M. (2012), “Preparation and application of barium sulfate nano-particles in the synthesis of 2, 4, 5-triaryl and N-aryl (alkyl)-2, 4, 5-triaryl imidazoles”, *Curr. Org. Synth.*, **9**(5), 727-732.
- Ghashang, M., Mansoor, S.S. and Aswin K. (2014), “Thiourea dioxide: An efficient and reusable organocatalyst for the rapid one-pot synthesis of pyrano [4, 3-b] pyran derivatives in water”, *Chin. J. Catal.*, **35**(1), 127-133.
- Ghashang, M., Kargar, M., Shafiee, M.R.M., Mansoor, S.S., Fazlinia, A. and Esfandiari, H. (2015), “CuO nano-structures prepared in rosmarinus officinalis leaves extract medium: Efficient catalysts for the aqueous media preparation of dihydropyran [3, 2-c] chromene derivatives”, *Recent Pat. Nanotech.*, **9**(3), 204-211.
- Ghosh, A., Saha, R., Mukherjee, K., Sar, P., Ghosh, S.K., Malik, S., Bhattacharyya, S.S. and Saha, B. (2014a), “Rate enhancement via micelle encapsulation for room temperature metal catalyzed Ce(IV) oxidation of *p*-chlorobenzaldehyde to *p*-chlorobenzoic acid in aqueous medium at atmospheric pressure”, *J. Mol. Liq.*, **190**, 81-93.
- Ghosh, A., Saha, R. and Saha, B. (2014b), “Effect of CHAPS and CPC micelles on Ir(III) catalyzed Ce(IV) oxidation of aliphatic alcohols at room temperature and pressure”, *J. Mol. Liq.*, **196**, 223-237.
- Ghosh, A., Sar, P., Malik, S. and Saha, B. (2015), “Role of surfactants on metal mediated cerium(IV) oxidation of valeranaldehyde at room temperature and pressure”, *J. Mol. Liq.*, **211**, 48-62.
- Jiang, J., Ai, L. and Li, L. (2009), “Synthesis and characterization of polyaniline-based nanocomposites containing magnetic Li-Ni-La ferrite”, *J. Non-Cryst. Solids*, **355**(34-36), 1733-1736.
- Jing, S., Xing, S., Lianxiang, Y., Yan, W. and Zhao, C. (2007), “Synthesis and characterization of Ag/polyaniline core-shell nanocomposites based on silver nanoparticles colloid”, *Mater. Lett.*, **61**(13), 2794-2797.
- Kargar, M., Mohammad Shafiee, M.R. and Ghashang, M. (2015), “Green protocol preparation of ZnO nanoparticles in prunus cerasus juice media”, *Nanosci. Nanotech.-Asia*, **5**(1), 44-49.
- Khened, B.S., Ambika Prasad, M.V.N. and Sasikala, M. (2016), “High sensitivity and selectivity of LPG gas by three dimensional molecular ordered polyaniline/CeO₂ nanocomposites”, *Sensor Lett.*, **14**(8), 786-793.
- Kowsari, E. and Faraghi, G. (2010), “Ultrasound and ionic-liquid-assisted synthesis and characterization, of polyaniline/Y₂O₃ nanocomposite with controlled conductivity”, *Ultrason. Sonochem.*, **17**(4), 718-725.
- Kumar, N.A. and Baek, J. (2014), “Electrochemical supercapacitors from conducting polyaniline-graphene platforms”, *Chem. Commun.*, **50**(48), 6298-6308.
- Kumar, E., Selvarajan, P. and Muthuraj, D. (2012), “Preparation and characterization of polyaniline/cerium dioxide (CeO₂) nanocomposite via in situ polymerization”, *J. Mater. Sci.*, **47**(20), 7148-7156.
- Lin, J., Zhang, C.G., Yan, Z., Zhu, Y., Peng, Z.W., Hauge, R.H., Natelson, D. and Tour, J.M. (2013), “3-dimensional graphene carbon nanotube carpet-based microsupercapacitors with high electrochemical performance”, *Nano Lett.*, **13**(1), 72-78.
- Mo, T.-C., Wang, H.-W., Chen, S.-Y. and Yeh, Y.-C. (2008), “Synthesis and dielectric properties of polyaniline/titanium dioxide nanocomposites”, *Ceram. Int.*, **34**(7), 1767-1771.
- Pech, D., Brunet, M., Durou, H., Huang, P., Mochalin, V., Gogotsi, Y., Taberna, P. and Simon, P. (2010), “Ultrahigh-power micrometre-sized supercapacitors based on inion-like carbon”, *Nat. Nanotechnol.*, **5**, 651-654.
- Phang, S.W., Tadokoro, M., Watanabe, J. and Kuramoto, N. (2008), “Microwave absorption behaviors of polyaniline nanocomposites containing TiO₂ nanoparticles”, *Curr. Appl. Phys.*, **8**(3-4), 391-394.
- Pillalamarri, S.K., Blum, F.D., Tokuhira, A.T. and Bertino, M.F. (2005), “One-pot synthesis of polyaniline-metal nanocomposites”, *Chem. Mater.*, **17**(24), 5941-5944.
- Poyraz, S., Cerkez, I., Huang, T., Liu, Z., Kang, L., Luo, J. and Zhang, X. (2014), “One-step synthesis and characterization of polyaniline nanofiber/silver nanoparticle composite networks as anti-bacterial agents”, *ACS Appl. Mater. Interfaces*, **6**(22), 20025-20034.
- Reddy, K.R., Lee, K.P. and Gopalan, A.I. (2008), “Self-assembly approach for the synthesis of electro-magnetic functionalized Fe₃O₄/polyaniline nanocomposites: Effect of dopant on the properties”, *Colloids Surf. A: Physicochem. Eng. Asp.*, **320**(1-3), 49-56.
- Sasikumar, Y., Madhan Kumar, A., Gasem, Z.M. and Ebenso, E.E. (2015), “Hybrid nanocomposite from aniline and CeO₂ nanoparticles: Surface protective performance on mild steel in acidic environment”, *Appl. Surf. Sci.*, **330**, 207-215.
- Shafiee, M.R.M., Fazlinia, A., Yaghooti, N. and Ghashang, M. (2012), “A convenient method for the preparation of 2, 4, 5-triaryl imidazoles using barium chloride dispersed on silica gel nanoparticles (BaCl₂-nano SiO₂) as heterogeneous reusable catalyst”, *Lett. Org. Chem.*, **9**(5), 351-355.
- Shafiee, M.R.M., Ghashang, M. and Fazlinia, A. (2013), “Preparation of 1, 4-dihydropyridine derivatives using perchloric acid adsorbed on magnetic Fe₃O₄ nanoparticles coated with silica”, *Curr. Nanosci.*, **9**(2), 197-201.
- Sharma, R.K., Sahu, V., Grover, S., Goel, S. and Singh, G. (2015), “Asymmetric supercapacitive characteristics of PANI embedded holey graphene nanoribbons”, *ACS Sustain. Chem. Eng.*, **3**(7), 1460-1469.
- Stejskal, J., Trchová, M., Prokeš, J. and Sapurina, I. (2001), “Brominated polyaniline”, *J. Chem. Mater.*, **13**(11), 4083-4086.
- Taghri, H., Ghashang, M. and Biregan, M.N. (2016), “Preparation of 1-amidoalkyl-2-naphthol derivatives using barium phosphate nano-powders”, *Chin. Chem. Lett.*, **27**(1), 119-126.
- Taguchi, M., Takami, S., Adschiri, T., Nakane, T., Sato, K. and Naka, T. (2011), “Supercritical hydrothermal synthesis of hydrophilic polymer-modified water dispersible CeO₂ nanoparticles”, *Cryst. Eng. Commun.*, **13**(8), 2841-2848.
- Tamboli, M.S., Kulkarni, M.V., Patil, R.H., Gade, W.N., Navale, S.C. and Kale, B.B. (2012), “Nanowires of silver-polyaniline nanocomposite synthesized via in situ polymerization and its novel functionality as an antibacterial agent”, *Colloids Surf. B*, **92**, 35-41.
- Tsai, H.L., Schindler, J.L., Kannewurf, C.R. and Kanatzidis, M.G. (1997), “Plastic superconducting polymer-NbSe₂ nanocomposites”, *Chem. Mater.*, **9**(4), 875-878.
- Weiss, Z., Mandler, D., Shustak, G. and Domb, A.J. (2004), “Pyrrole derivatives for electrochemical coating of metallic medical devices”, *J. Polym. Sci. A: Polym. Chem.*, **42**(7), 1658-1667.
- Xiong, S., Phua, S.L., Dunn, B.S., Ma, J. and Lu, X. (2010), “Covalently bonded polyaniline-TiO₂ hybrids: A facile approach to highly stable anodic electrochromic materials with low oxidation potentials”, *Chem. Mater.*, **22**(1), 255-260.
- Yan, Y., Cheng, Q., Pavlinek, V., Saha, P. and Li, C. (2012), “Fabrication of polyaniline/mesoporous carbon/MnO₂ ternary nanocomposites and their enhanced electrochemical performance for supercapacitors”, *Electrochim. Acta*, **71**, 27-32.
- Zhang, X., Goux, W.J. and Manohar, S.K. (2004), “Synthesis of polyaniline nanofibers by nanofiber seeding”, *J. Am. Chem. Soc.*, **126**(14), 4502-4503.
- Zhou, H., Lin, Y., Yu, P., Su, L. and Mao, L. (2009), “Doping polyaniline with pristine carbon nanotubes into electroactive

nanocomposite in neutral and alkaline media”, *Electrochem. Commun.*, **11**(5), 965-968.

Zhou, C., Zhang, Y., Li, Y. and Liu, J. (2012), “Construction of high capacitance 3D CoO @ polypyrrole nanowire array electrode for aqueous asymmetric supercapacitor”, *Nano Lett.*, **13**(5), 2078-2085.

CC